

Surface Outflow in Optically Thick Dust Disks by the Radiation Pressure ¹

Taku Takeuchi and D. N. C. Lin

UCO/Lick Observatory, University of California, Santa Cruz, CA95064

taku@ucolick.org, lin@ucolick.org

ABSTRACT

We study the outflow of dust particles on the surface layers of optically thick disks. At the surface of disks around young stars, small dust particles (size $\lesssim 10 \mu\text{m}$) experience stellar radiation pressure support and orbit more slowly than the surrounding gas. The resulting tail-wind imparts energy and angular momentum to the dust particles, moving them outward. This outflow occurs in the thin surface layer of the disk that is exposed to starlight, and the outward mass flux is carried primarily by particles of size $\sim 0.1 \mu\text{m}$. Beneath the irradiated surface layer, dust particles experience a head-wind, which drives them inward. For the specific case of a minimum-mass-solar-nebula, less than a thousandth of the dust mass experiences outward flow. If the stellar luminosity is 15 times brighter than the sun, however, or if the gas disk mass is as small as $\sim 100M_{\oplus}$, then the surface outflow can dominate the inward flux in certain radial ranges, leading to the formation of rings or gaps in the dust disks.

Subject headings: accretion, accretion disks — planetary systems: formation — solar system: formation

1. Introduction

Circumstellar disks around young stars are composed of gas and dust particles, and in general, the dust and gas accretion velocities are not equal. The gas suffers turbulent viscosity and accretes onto the central star on a viscous time-scale of order $10^6 - 10^7$ yr (Hartmann et al. 1998). The orbital evolution of dust particles, on the other hand, is controlled by gas drag (Adachi, Hayashi, & Nakazawa 1976; Weidenschilling 1977).

Several factors affect the radial motion of particles. First, gas drag in the radial direction entrains particles in the accretion flow. When the gas density is high or when the particle size is small, the particles follow the gas motion, and accrete onto the star on the viscous time-scale. Second, angular momentum is transferred between particles and the gas. The radial gas pressure gradient shifts the angular velocity of the gas slightly from the Keplerian value. Moreover, if starlight can ir-

radiate particles, then radiation pressure causes non-Keplerian deviations in the particle velocity as well. Dust particles can thus gain or lose angular momentum through gas drag and thus move outward or inward, depending on whether they experience a net head-wind or a net tail-wind.

In a previous paper (Takeuchi & Lin 2002, hereafter Paper I), we studied particle motion in optically thick disks, using the assumption that radiation pressure on the dust is negligible. We found that dust particles smaller than $10 \mu\text{m}$ accrete with smaller velocity than the gas. As the gas accretion proceeds, small dust particles are left behind in the disk and the dust-to-gas ratio gradually increases. Because circumstellar disks associated with young stars are generally optically thick, the majority of dust particles are not directly exposed to the stellar radiation, and the approximation used in Paper I is applicable. There are always, however, some particles near the disk surfaces that are directly irradiated, and the motion of such particles are affected by radiation pressure. Klahr & Lin (2001) and Takeuchi & Artymow-

¹To appear in Aug. 10 issue of *Astrophys. J.*

icz (2001) studied the motion of particles in optically thin gas disks around young Vega-type stars, where the dust experiences both gas drag and radiation pressure. Because the radiation pressure reduces the angular velocity of the dust below that of the gas, the dust tends to move outward. Thus, in a more refined description of an optically thick disk, one expects that particles in the irradiated surface layer move outward, while beneath the surface layer particles move inward. If the surface outflow dominates the midplane inflow, then there is a net radial expansion that may induce the formation of rings or gaps.

In this paper, we study the surface dust outflow in optically thick disks due to radiation pressure. The mass flux of the surface outflow is calculated, which is compared to that of the inflow inside the disk. We find that the surface outflow is negligible in a minimum-mass-solar-nebula model, but that the surface outflow can dominate inflow at some disk radii in some cases, including situations involving high stellar luminosity or low gas mass. In such disks, the appearance of rings or gaps is expected.

2. The Distribution of the Gas and the Dust

2.1. The Gas Disk

We consider circumstellar disks around young pre-main-sequence stars. The disks are turbulent and are accreting onto the central stars, but they are assumed to be passive, that is, the disks are primarily heated by stellar radiation only. When turbulent fluctuations are averaged out, the mean gas motion is nearly in hydrostatic equilibrium and the radial accretion flow is much slower than the azimuthal Kepler rotation. In cylindrical coordinates (r, θ, z) , the balance of forces in the r - and z -directions are

$$r\Omega_g^2 - \frac{GMr}{(r^2 + z^2)^{3/2}} - \frac{1}{\rho_g} \frac{\partial P_g}{\partial r} = 0, \quad (1)$$

$$-\frac{GMz}{(r^2 + z^2)^{3/2}} - \frac{1}{\rho_g} \frac{\partial P_g}{\partial z} = 0, \quad (2)$$

where Ω_g is the gas angular velocity, M is the central star's mass, ρ_g is the gas density, and P_g is the gas pressure. For simplicity, we assume that the gas disk has power-law density and temperature

profiles in the radial direction, and is isothermal in the vertical direction. The temperature distribution is written as a power-law of index q ,

$$T(r, z) = T_0 r_{\text{AU}}^q, \quad (3)$$

where the subscript “0” denotes quantities at 1 AU, and a non-dimensional quantity r_{AU} is the radius in AU. The isothermal sound speed is $c = c_0 r_{\text{AU}}^{q/2}$ and the gas disk scale height is thus defined as

$$h_g(r) \equiv \frac{c}{\Omega_{\text{K,mid}}} = h_0 r_{\text{AU}}^{(q+3)/2}, \quad (4)$$

where $\Omega_{\text{K}} = [GM/(r^2 + z^2)^{3/2}]^{1/2}$ is the Keplerian angular velocity and the subscript “mid” indicates the midplane value. From the balance between the stellar gravity and the gas pressure gradient in the z -direction (eq. [2]), we have the density distribution

$$\rho_g(r, z) = \rho_0 r_{\text{AU}}^p \exp\left(-\frac{z^2}{2h_g^2}\right), \quad (5)$$

where a power-law in r is assumed. The surface density of the gas disk is given by

$$\Sigma_g(r) = \int_{-\infty}^{+\infty} \rho_g dz = \sqrt{2\pi} \rho_0 h_0 r_{\text{AU}}^{p_s}, \quad (6)$$

where $p_s = p + (q + 3)/2$. The angular velocity Ω_g of the gas is slightly different from the Keplerian angular velocity Ω_{K} because of the radial pressure gradient in the gas. From equation (1), we have

$$\Omega_g^2(r, z) = (1 - \eta) \Omega_{\text{K}}^2(r, z), \quad (7)$$

where $\eta = -(r\Omega_{\text{K}}^2 \rho_g)^{-1} \partial P_g / \partial r$ is the ratio of the gas pressure gradient to the stellar gravity in the radial direction. As derived in equation (17) in Paper I, η is written to order $(h_g/r)^2$ as

$$\eta = -\left(\frac{h_g}{r}\right)^2 \left(p + q + \frac{q + 3}{2} \frac{z^2}{h_g^2}\right). \quad (8)$$

The disk has a turbulent viscosity ν . Turbulent disk viscosity has been ascribed to various mechanisms, including the convective instability (Lin & Papaloizou 1980) and the magneto-rotational instability (Balbus & Hawley 1991). In this paper, we simply model the viscous effect of turbulence using the so-called α prescription (Shakura & Sunyaev 1973),

$$\nu = \alpha c h_g = \alpha c_0 h_0 r_{\text{AU}}^{q+3/2}. \quad (9)$$

We adopt the following fiducial parameters: $M = 1 M_\odot$, $\rho_0 = 2.83 \times 10^{-10} \text{ g cm}^{-3}$, $h_0 = 3.33 \times 10^{-2} \text{ AU}$, $p = -2.25$, $q = -0.5$, and $\alpha = 10^{-3}$. These values correspond to a disk having a gas mass of $2.5 \times 10^{-2} M_\odot$ inside 100 AU. The power law index of the surface density is $p_s = p + (q + 3)/2 = -1.0$. The temperature distribution is $T = 278 r_{\text{AU}}^{-1/2} \text{ K}$.

2.2. The Dust Disk

2.2.1. Radial Distribution

The radial surface density distribution of the dust is assumed to be proportional to that of the gas disk, so that $\Sigma_{d,\text{all}}(r) = f_{\text{dust}} \Sigma_g(r)$, where the constant f_{dust} is the dust-to-gas mass ratio. Throughout the paper, we adopt the value $f_{\text{dust}} = 0.01$ at all radii. The subscript ‘‘all’’ represents contributions from the entire distribution of particle sizes. In this paper, we consider cases where all particles have the same size and also power-law size distributions. For power-law size distributions, the size range is bracketed at the large and small ends, $[s_{\text{min}}, s_{\text{max}}]$. We adopt a power-law index -3.5 , appropriate to the distribution expected following collisional evolution (Hellyer 1970). The surface number density of particles in a size range $[s, s + ds]$ at a distance r from the star is given by

$$N_\Sigma(r, s) ds = N_1(r) s_{\text{cm}}^{-3.5} ds, \quad (10)$$

where s_{cm} is the particle size in centimeters. The radial distribution of particles N_1 is

$$N_1(r) = \frac{3}{8\pi\rho_p} f_{\text{dust}} \Sigma_g(r) \left(s_{\text{max,cm}}^{1/2} - s_{\text{min,cm}}^{1/2} \right)^{-1} (\text{cm})^{-4}, \quad (11)$$

where ρ_p is the physical density of a particle. We adopt $\rho_p = 1.25 \text{ g cm}^{-3}$, $f_{\text{dust}} = 0.01$, $s_{\text{min}} = 0.01 \text{ }\mu\text{m}$, and $s_{\text{max}} = 1 \text{ }\mu\text{m}$.

2.2.2. Vertical Distribution

Dust particles feel the z -component of the stellar gravity, and thus sediment toward the disk midplane. Small particles ($s \lesssim 1 \text{ cm}$) immediately (within one orbit) reach the terminal velocity $v_{z,d}$, where the gravity and the gas drag are in balance. For small particles considered here ($s \lesssim 1 \text{ cm}$), the Epstein’s drag law is applied, because the mean free path of the gas molecules (7 cm at 1 AU) is larger than the particle size. The gas drag force is

$$\mathbf{F}_g = -\frac{4}{3}\pi\rho_g s^2 v_t (\mathbf{v}_d - \mathbf{v}_g), \quad (12)$$

where v_t is the mean thermal velocity of the gas molecules, and \mathbf{v}_d and \mathbf{v}_g are the velocities of the dust and the gas, respectively. The stopping time due to the gas drag is $t_s = m_d |\mathbf{v}_d - \mathbf{v}_g| / |\mathbf{F}_g|$, where $m_d = \frac{4}{3}\pi\rho_p s^3$ is the particle mass. We define the non-dimensional stopping time normalized by the orbital time as,

$$T_s = t_s \Omega_{\text{K,mid}} = \frac{\rho_p s v_{\text{K,mid}}}{\rho_g r v_t}, \quad (13)$$

where $v_{\text{K,mid}}$ is the Keplerian velocity at the midplane. When terminal velocity is achieved, the gas drag balances the z -component of the stellar gravity, $-m_d \Omega_{\text{K}}^2 z$. Using the approximation $\Omega_{\text{K}} \approx \Omega_{\text{K,mid}}$, the terminal velocity $v_{z,d}$ is

$$v_{z,d} = -\Omega_{\text{K,mid}} T_s z. \quad (14)$$

The mass flux of particles in the vertical direction is

$$f_{z,\text{sed}} = \rho_d v_{z,d}, \quad (15)$$

where ρ_d is the dust mass density. If the gas disk were laminar, the particles would concentrate at the midplane in a time that is short compared to the evolution time of the gas disk (the sedimentation time-scale is about 10^6 yr for $1 \text{ }\mu\text{m}$ particles at 10 AU). When the gas disk is turbulent, however, the gas stirs and disperses the particles and prevents sedimentation. The mass flux of dust arising from this turbulent diffusion is assumed proportional to the gradient of the dust concentration ρ_d/ρ_g in analogy with molecular diffusion (e.g, Monin & Yaglom, 1971, p. 579; Morfill, 1985, §3.5.1; Cuzzi, Dobrovolskis, & Champney 1993). In the vertical direction, the mass flux $f_{z,\text{dif}}$ is

$$f_{z,\text{dif}} = -\frac{\rho_g \nu}{\text{Sc}} \frac{\partial}{\partial z} \left(\frac{\rho_d}{\rho_g} \right), \quad (16)$$

where the Schmidt number, Sc , represents the coupling strength between the particles and the gas. For small particles that are well coupled to the gas, Sc approaches unity. For large particles that are decoupled from the gas, Sc becomes infinite. In our standard model, we use $\text{Sc} = 1$.

In equilibrium, the sedimentation mass flux balances the diffusive mass flux:

$$f_{z,\text{sed}} + f_{z,\text{dif}} = 0. \quad (17)$$

The equilibrium dust density distribution is given by equation (31) in Paper I. For particles in a size

range $[s, s + ds]$, the density distribution is

$$\begin{aligned} \rho_d(r, z, s)ds &= \rho_d(r, 0, s) \exp\left[-\frac{z^2}{2h_g^2}\right] \\ &- \frac{ScT_{s,\text{mid}}}{\alpha} \left(\exp\frac{z^2}{2h_g^2} - 1\right) ds, \end{aligned} \quad (18)$$

where $T_{s,\text{mid}}$ is the midplane value of the non-dimensional stopping time. The total dust density is

$$\rho_{d,\text{all}}(r, z) = \int_{s_{\text{min}}}^{s_{\text{max}}} \rho_d(r, z, s) ds. \quad (19)$$

As discussed in Paper I, the sedimentation of particles is more effective for larger particles and at larger distances from the star. As increasing the distance, the dust disk becomes relatively thinner compared to the gas disk.

2.3. Optical Depth from the Star

The disks considered in this paper are optically thick at visible wavelengths even in the vertical direction ($\tau_{\text{ver}} \sim 100$ at 100 AU). Stellar light cannot penetrate the dust disk. Only particles residing in the thin surface layer are exposed to stellar radiation pressure.

The optical depth from the star to the position (r, z) in the dust disk is

$$\tau(r, z) = \int_{r_{\text{in}}}^r \frac{\kappa}{f_{\text{dust}}} \rho_{d,\text{all}}(r', z') \sqrt{1 + \frac{z^2}{r'^2}} dr', \quad (20)$$

where $z' = (z/r)r'$, r_{in} is inner edge of the dust disk, and κ is the dust opacity in the visible wavelength for an unit mass of the gas. The opacity for a unit mass of the dust is κ/f_{dust} . In our calculations, we adopt $r_{\text{in}} = 0.1$ AU. This choice of inner boundary does not affect the integral (20), because the dust disk is flared and the main contribution to the optical depth comes from the dust at relatively large distances from the star. We adopt a dust mass opacity $\kappa = 100 \text{ cm}^2 \text{ g}^{-1}$ for visible wavelengths. For particles smaller than $100 \mu\text{m}$, the opacity is independent of (the maximum) particle size (see Figs. 5 and 11 in Miyake & Nakagawa 1993). Thus, we need not consider variations in κ with changes in the particle size.

Figure 1 shows the disk surfaces at which the optical depth to the starlight is unity. Above these

illuminated surfaces, the dust particles are directly exposed to the stellar radiation. Figure 1a shows the illuminated surfaces of the standard disk models which are composed of single-sized particles (0.1 to $10 \mu\text{m}$). As the particle size increases, the level of the illuminated surfaces becomes lower. This size dependence is because larger particles sediment more readily, and thus concentrate near the midplane. The illuminated surfaces have a slightly flatter geometry than the gas disk, because the dust particles at larger distances sediment more effectively. Figure 1b shows the illuminated surfaces of the models containing power-law size distributions. The illuminated surfaces lie at roughly three disk scale heights, which are similar to those of the single-sized $0.1 \mu\text{m}$ particles. The location of the illuminated surface does not change significantly with the maximum size of the particles, because high altitude above the midplane is mostly populated by the smallest particles.

3. Outflow in the Surface Layer

Dust particles above the illuminated surface suffer radiation pressure from the central star. The radiation pressure balances a part of the stellar gravity, so that the small particles orbit slower than the gas. Because the gas drag transfers angular momentum from the gas to the particles, the particles move outward, leading to an outflow in the surface layers of dust disks. In this section, we estimate the mass fluxes carried by these outflows.

3.1. Outflow Mass Flux

The radiation pressure is expressed through the ratio β to the stellar gravity. The radial component is

$$F_{\text{rad}} = \beta m_d r \Omega_K^2. \quad (21)$$

The value of β , which is calculated with the Mie's scattering theory, depends on the particle composition, porosity, shape, and size. In this paper, we adopt β for ‘‘young cometary particles,’’ which is calculated by Wilck & Mann (1996) for typical interplanetary particles in the solar system and shown in Figure 2. In general, stellar light causes Poynting-Robertson drag on the particles in addition to the gas drag induced by radiation pressure. However, in the gas disks considered here, the gas density is sufficiently large so that gas drag dominates Poynting-Robertson drag (see the discussion

in Takeuchi & Artymowicz 2001, §4.2). Poynting-Robertson drag can therefore be neglected.

The equations of motion of a particle are

$$\frac{dv_{r,d}}{dt} = \frac{v_{\theta,d}^2}{r} - (1 - \beta)\Omega_K^2 r - \frac{\Omega_{K,\text{mid}}}{T_s}(v_{r,d} - v_{r,g}), \quad (22)$$

$$\frac{d}{dt}(rv_{\theta,d}) = -\frac{v_{K,\text{mid}}}{T_s}(v_{\theta,d} - v_{\theta,g}), \quad (23)$$

where v_r and v_θ are the r - and θ - components of the velocity, and the subscripts “ g ” and “ d ” distinguish gas and dust. As in Paper I, we assume $v_{\theta,g} \approx v_{\theta,d} \approx v_{K,\text{mid}}$ and $d(rv_{\theta,d})/dt \approx v_{r,d}d(rv_{K,\text{mid}})/dr = v_{r,d}v_{K,\text{mid}}/2$. From equation (23) we then have

$$v_{\theta,d} - v_{\theta,g} = -\frac{1}{2}T_s v_{r,d}. \quad (24)$$

In equation (22), $dv_{r,d}/dt = O(v_{r,d}^2/r)$ is neglected if $(v_{r,d}/v_{K,\text{mid}})^2 \ll 1$. We also neglect second order terms in η and $(v_{\theta,d} - v_{\theta,g})/v_{K,\text{mid}}$. To this level of approximation, $v_{\theta,d}^2 \approx v_{\theta,g}^2 + 2v_{\theta,g}(v_{\theta,d} - v_{\theta,g}) \approx v_K^2(1 - \eta) + 2v_{K,\text{mid}}(v_{\theta,d} - v_{\theta,g})$, and equation (22) becomes

$$(\beta - \eta)v_K^2 + 2v_{K,\text{mid}}(v_{\theta,d} - v_{\theta,g}) - \frac{v_{K,\text{mid}}}{T_s}(v_{r,d} - v_{r,g}) = 0. \quad (25)$$

Using equation (24) and $v_K \approx v_{K,\text{mid}}$, the particle radial velocity is

$$v_{r,d}(r, z, s) = \frac{T_s^{-1}v_{r,g} + (\beta - \eta)v_{K,\text{mid}}}{T_s + T_s^{-1}}. \quad (26)$$

The value of η is of order $(h_g/r)^2$ and it is smaller than 0.05. Since particles smaller than $10 \mu\text{m}$ have $\beta \gg \eta$ (see Fig. 2), η in equation (26) can be neglected. Particles larger than $\sim 100 \mu\text{m}$ may have β smaller than η . For such large particles, the radiation pressure is unimportant, even if they are above the illuminated surface. In this section, we consider only small particles with radii less than $10 \mu\text{m}$. Such particles have non-dimensional stopping times $T_s \ll 1$ (see Fig. 2 in Paper I). The radial velocity then reduces to

$$v_{r,d} = v_{r,g} + \beta T_s v_{K,\text{mid}}. \quad (27)$$

The mass flux of the outflow in the surface layer is

$$F_{\text{sur}}(r) = \int_{s_{\text{min}}}^{s_{\text{max}}} 2 \int_{z_{\text{sur}}}^{\infty} 2\pi r \rho_d(r, z, s) v_{r,d}(r, z, s) dz ds, \quad (28)$$

where z_{sur} is the height of the illuminated surface. The factor 2 arises from considering both the top and bottom surfaces. In the integration in z above the illuminated surface, $v_{r,d}$ varies less rapidly than ρ_d , and we may use its value at the illuminated surface. The mass flux is then expressed as

$$F_{\text{sur}}(r) = 2\pi r \int_{s_{\text{min}}}^{s_{\text{max}}} v_{r,d}(r, z_{\text{sur}}, s) \Sigma_{d,\text{sur}}(r, s) ds, \quad (29)$$

where $\Sigma_{d,\text{sur}} ds$ is the surface density of dust particles above the illuminated surface in the size range $[s, s + ds]$,

$$\Sigma_{d,\text{sur}}(r, s) = 2 \int_{z_{\text{sur}}}^{\infty} \rho_d(r, z, s) dz. \quad (30)$$

The surface outflow can clear out the dust within a distance r from the star on a time-scale $t_{\text{out}} \approx M_{\text{dust}}(r)/F_{\text{sur}}(r)$, where $M_{\text{dust}}(r)$ is the dust mass within r . In our models, the disk mass is dominated by the outermost part of the disk and $M_{\text{dust}}(r) \approx \pi r^2 \Sigma_{d,\text{all}}(r)$. The dust clearing (or the disk evolution) time-scale is thus

$$t_{\text{out}}(r) \approx \frac{\pi r^2 \Sigma_{d,\text{all}}(r)}{F_{\text{sur}}(r)}. \quad (31)$$

While at the surface layer particles flow outward, the particles beneath the surface layer are shielded from stellar irradiation. At such locations, the gas drag causes a net inward flow of particles as shown in Paper I. From equation (26) with $\beta = 0$, the radial velocity of particles beneath the surface layer is

$$v_{r,d}(r, z, s) = \frac{T_s^{-1}v_{r,g} - \eta v_{K,\text{mid}}}{T_s + T_s^{-1}}. \quad (32)$$

The mass flux is

$$F_{\text{in}} = \int_{s_{\text{min}}}^{s_{\text{max}}} \int_{-z_{\text{sur}}}^{z_{\text{sur}}} 2\pi r \rho_d(r, z, s) v_{r,d}(r, z, s) dz ds. \quad (33)$$

The time required for the inflow to transport a mass equal to the dust mass within r is

$$t_{\text{in}}(r) \approx \frac{\pi r^2 \Sigma_{d,\text{all}}(r)}{|F_{\text{in}}(r)|}. \quad (34)$$

We define this as the disk evolution time through the inflow. This definition of t_{in} does not mean the

time for carrying the total dust mass outside r to the inner part, but it is convenient for comparing with t_{out} . Comparison of t_{out} and t_{in} simply means comparison of the outflow and inflow fluxes. The disk clearing through the surface outflow occurs effectively only if the surface flux is stronger than the inflow flux, i.e., $t_{\text{out}} < t_{\text{in}}$. The comparison of these two time-scales is discussed in §3.3 and §3.4 below.

3.2. Evolution Time of the Disks through the Outflow

We first discuss the disk clearing time, t_{out} , through the surface outflow. In this subsection, we adopt the assumption that inflow flux near the midplane is negligible and that only the surface flow affects the dust structure within the disk. In §3.3 and §3.4, we relax this assumption and consider more realistic scenarios including the effects of inflow near the midplane.

The particles in the surface layer have outflow velocity, $v_{r,d}(r, z_{\text{sur}}, s)$. These particles are blown from their orbits to larger radii on a time-scale $t_b = r/v_{r,d}(r, z_{\text{sur}}, s)$. For disks composed of single-sized particles, t_b is plotted in Figure 3. The blow-off time for 0.1 to 10 μm particles is about 10^2 yr at a few AU from the star, and is about 10^5 yr at 100 AU. The blow-off time is much shorter than the inward migration time inside the disk, which is discussed in §3.3 below, because $\beta \gg \eta$ and because the stopping time T_s at the illuminated surface is much longer than at the midplane.

In our standard model, the dust disk is highly optically thick. Even in the vertical direction at 100AU, the optical depth is $\tau_{\text{ver}} \sim 100$, so the layer above the illuminated surface is very thin. Figure 4 shows the ratio of the surface density of the layer to that of the whole disk ($\Sigma_{d,\text{sur,all}}/\Sigma_{d,\text{all}}$). As the distance from the star increases, the mass ratio increases and the surface layer becomes thicker. However, even at 100 AU, the mass of the surface layer is less than 10^{-3} times the dust disk mass. In the case of single-sized particles (Fig. 4a) the mass of the surface layer is smaller for disks with larger particle sizes. As the particles grow larger, they sediment more to the midplane, and the surface layer becomes thinner. On the other hand, for the mixed-sized particles (Fig. 4b), the mass of the surface layer does not vary significantly with the maximum size. Because smaller particles exist at

higher altitudes above the midplane, the surface layer is composed mainly of the smallest particles, and the quantity of smallest particles in the surface layer does not vary with the maximum size.

Although Figure 3 implies that the outflow velocity at the surface layer is high, the outflow mass flux is not large because of the small mass contained in the surface layer. The disk evolution time t_{out} through the surface outflow is shown in Figure 5a. The evolution time of the disk composed of 0.1 μm particles is about 10^7 yr at 1 AU and 10^8 yr at 100 AU. Thus, in 10^7 yr, the dust outflow mass which has passed 1 AU becomes comparable to the dust disk mass inside 1 AU. If the radial motion of the dust disk occurs only through surface outflow, the particles in the innermost part of the disk will escape from the region inside 1 AU in 10^7 yr, and a hole will appear. The hole expands, and in 10^8 yr, the radius of the hole reaches 100 AU. There is, however, an accretion flow under the surface layer. Inhibition of disk clearing by the accretion flow is discussed in §3.3 below. As the particle size increases, the evolution time increases as well. This is because particles with larger sizes concentrate more at the midplane and the surface layer becomes thinner. The blow-off time t_b for a larger particle at its surface layer is also larger because of the higher local density of the gas at the lower surface layer (Fig. 3). If the disk is composed of 10 μm particles, it takes about 10^9 yr for a disk of radius 100 AU to evolve.

Figure 5b shows the evolution times for disks composed of mixed-sized particles. The disk containing [0.01 μm – 1 μm] particles evolves in about 3×10^7 yr at 1 AU and in 3×10^8 yr at 100 AU. The disk evolution occurs mainly through the outflow of 0.1 μm particles. While the surface layer is composed primarily of the smallest (0.01 μm) particles, these particles do not receive radiation pressure as effectively as particles with 0.1 μm (see Fig. 2). Thus, the surface outflow is mainly carried by a minor fraction of particles in the 0.1 μm range, and the disk evolution time of the mixed-sized particles is much longer than that of the disk with the single-sized particles of 0.1 μm . The evolution time increases with the maximum particle size. The dependence of the maximum size on the evolution time, however, is not as significant as in the case of single-sized particles. For disks composed of mixed-sized particles, particles of size

0.1 μm form the main contribution to the surface outflow. The number density of 0.1 μm particles decreases as the maximum particle size increases. However, because the thickness of the surface layer is determined by the optical depth from the star and the opacity comes mainly from 0.1 μm particles, the total mass of 0.1 μm particles in the surface layer does not change significantly (Fig. 4*b*). Hence, the outflow flux maintains a relatively constant value.

3.3. Comparison with the Inward Migration Time

The surface outflow leads to disk clearing only if it dominates the under-surface inflow. The disk evolution time-scale, t_{in} , through the inflow is shown as the dashed lines in Figure 5. As discussed in Paper I, for sufficiently small particles that are well coupled to the gas, the inflow velocity is similar to the accretion velocity of the gas. In the standard model, particles smaller than 1 μm have velocities nearly indistinguishable from the gas throughout the disk. Particles of 10 μm decouple from the gas motion at large distances ($r \gtrsim 50$ AU) and have a shorter evolution time than the gas and smaller particles. The inflowing mass flux is much larger (10 times or more) than the mass flux of the surface outflow even for 0.1 μm particles. Therefore, the net mass flux of particles is dominated by the inflow beneath the surface layer. In the disks composed of mixed-sized particles (Fig. 5*b*), the inflow also dominates the net flow. The surface outflow has a very minor effect on the disk evolution in our standard model, regardless of the particle size.

3.4. Various Models

In our standard model, the surface outflow is negligible for disk evolution compared to the inflow inside the disk. This flow outcome is due to the surface layer being very thin such that its mass is a small fraction of the entire dust disk mass. The surface outflow may be important under some conditions where the surface layer is thicker or the outflow is much faster than the standard model. In this subsection, we consider several models to see under which conditions the surface outflow is important.

3.4.1. High Luminosity

Massive young stars have a larger luminosity-mass ratio. For example, $2.5M_{\odot}$ stars have about $20L_{\odot}/M_{\odot}$ for $\sim 10^7$ yr (D’Antona & Mazzitelli 1994). Under such a high luminosity-mass ratio, the dust particles are exposed to a stronger radiation pressure (β is proportional to L/M). Figure 6*a* shows the evolution time of the disk in the case where the stellar luminosity-mass ratio is 15 times larger than the standard model. The outflow velocity is 15 times faster than in the standard model, causing the outflow mass flux to dominate the inflow at large distances ($r \gtrsim 200$ AU). In this model, dust particles which are initially outside 200 AU are expelled to larger distances, while particles inside 200 AU are accreted onto the star. It is expected that a gap around 200 AU forms in 10^7 yr.

3.4.2. Small Disk Mass

If the total dust mass is smaller, the disk optical depth is smaller so that the layer above the illuminated surface is thicker. Figure 6*b* shows the evolution time of the disks whose masses are 0.1 and 0.01 times smaller than the standard disk. The mass flux of the surface outflow is almost independent of the disk mass because the mass of the surface layer, which is determined by the optical thickness, is approximately constant. Therefore, the relative importance of the surface outflow, which is proportional to the mass ratio of the surface layer to the whole disk, increases with decreasing the total dust mass. The evolution time through the inflow (see the dashed lines) at the inner part of the disk is similar to that of the standard model, while at the outer part it decreases with decreasing disk mass. As the disk mass decreases, the gas density at the outer region of the disk becomes insufficient to keep dust particles moving together with the gas. The inward drift velocity of particles relative to the gas becomes faster for disks with smaller gas mass. For such drifting particles, the evolution time is proportional to $r^{2+p-q/2}$ (see Paper I, §3.3.3), which is constant with r in our models ($p = -2.25$ and $q = -0.5$). For the disk with one tenth the mass as the standard model, the evolution time through the surface outflow is still longer than that of the inflow. If the disk is 10^{-2} times smaller than the

standard model (the gas mass inside 100 AU is $2.5 \times 10^{-4} M_{\odot} = 83 M_{\oplus}$), the surface outflow flux is comparable to the inflow flux at around 20 AU. Thus, there is no net flow at radii in the neighborhood of 20 AU. The dust particles initially outside 20 AU move inward until their migration is terminated at 20 AU. At the same time, the particles initially inside 20 AU continue to move inward and accrete onto the star. Therefore, the particle migration induces accumulation of dust at 20 AU and forms a ring there. Gas disks around young stars are expected to dissipate in 10^7 yr (Hartmann et al. 1998). When the gas mass is reduced to about $100 M_{\oplus}$, a ring appears at a radius of a few tens of AU.

3.4.3. High Diffusivity of Dust

In the standard model, the diffusivity of dust particles subject to turbulent motion of the gas is assumed to be the same as the diffusivity of the gas, i.e., the Schmidt number, Sc , is unity. Experiments show that Sc can be as small as 0.1 and dust particles are much more diffusive than the gas, if the Stokes number, St , is of order 10^{-2} (e.g., Fig. 1 in Cuzzi et al. 1993). The Stokes number is considered to be of the same order as the non-dimensional stopping time T_s . At radii of several hundred AU, $T_s \sim 10^{-2}$ for $0.1 \mu\text{m}$ particles at the illuminated surface ($z \sim 3h_g$). Thus, it is expected that such particles will spread to higher altitude, where they are easily blown off. Figure 6c shows the evolution time for such particles with $Sc = 0.1$. The dust particles are more diffusive and are stirred up to higher altitude by turbulence than in the case of $Sc = 1$. The illuminated surface is located higher, where the gas density is lower and the outflow velocity is faster. The outflow mass flux, however, is still smaller than the inflow mass flux within $r \lesssim 500$ AU. Inflow under the surface layer dominates even for the particles with high diffusivity.

3.4.4. Particle Growth

In the above discussion, we mainly used models which have a power-law size distribution with a maximum size of $1 \mu\text{m}$. The dust particles in circumstellar disks may have evolved to sizes larger than $1 \mu\text{m}$ (Beckwith & Sargent 1991; Mannings & Emerson 1994; D'Alessio, Calvet, & Hartmann 2001). Figure 5b shows the evolution time of the

disks as the maximum size of the particles is varied. The evolution time through the surface outflow does not change significantly as discussed in §3.1. The evolution time through inflow inside the disk, however, rapidly decreases with the growth of particles. At the outer part of the disk where the gas density is insufficient to keep the largest particles moving together with the gas, the inflow velocity of the particles is proportional to their size. For the size distribution with a power-law index -3.5 , the dust mass is dominated by the largest particles, and the inflow mass flux is proportional to the size of the largest particle. The evolution time through the inflow is as small as 10^5 yr when the largest particle is 1 mm, which is much shorter than that through the surface outflow. As the particles grow larger, the surface outflow becomes less important for the overall disk evolution.

4. Discussion and Summary

4.1. Progress in the Disk Evolution

We compared the surface outflow flux to the under-surface inflow flux and discussed conditions for disk clearing. In those comparisons, we assumed the dust density profiles described in §2, and neglected time variations of the dust density. In real disks, however, the dust density varies as the surface outflow proceeds. We discuss how density changes affect the subsequent evolution.

As dust particles above the illuminated surface are blown off by the stellar radiation, new particles continually diffuse into and replenish this region from below. The diffusion time over which the surface layer is re-populated is

$$t_{\text{rp}} \approx \frac{Sc(3h_g)^2}{\nu} \approx \frac{9}{\alpha} \Omega^{-1} \approx 10^3 r_{\text{AU}}^{3/2} \text{ yr}, \quad (35)$$

where we use the fact that the distance between the surface layer and the midplane is about three disk scale heights for $\alpha = 10^{-3}$ and $Sc = 1$. The diffusion time (10^6 yr at 100 AU) is much shorter than the disk evolution time t_{out} . Thus during the disk evolution, the dust in the surface layer is continuously replenished, and the surface outflow continues until the dust in the midplane is depleted.

In disks composed of mixed-sized particles, small ($s \lesssim 0.1 \mu\text{m}$) particles constitute the majorities of the surface outflow. The small particles

are rapidly removed from the disk, and are continuously replenished through the collisional destruction of larger particles. The collisional time scale, $t_{\text{col}} = (\pi s^2 n_d v_{\text{rel}})^{-1}$, where n_d is the particle number density and v_{rel} is the relative velocity of particles, is much shorter than the disk evolution time. For example, if we assume that the majority of the dust is composed of 1 cm particles, the relative velocity is about 10 cm s⁻¹ at 1 AU (from Fig. 3 in Weidenschilling & Cuzzi 1993), and the collisional time is $t_{\text{col}} \sim 10^3$ yr. If the dust is composed of smaller particles, the collisional time is smaller. The outcome of the collisions, however, is not well understood, and we do not know how many small particles are produced through the collisional destruction. In this paper, we simply assume that the particle size distribution is in an equilibrium state. The minimum size, the maximum size, and the power-law index of the distribution do not vary with time. In a realistic situation, however, at least the maximum size would grow with time, leading to inhibition of the disk clearing, as discussed in §3.4.4. Calculations that take account of dust growth are needed to solve this issue.

Because the disk evolution time t_{out} is shorter at smaller radii, the dust outflow proceeds from the inner disk. The particles blown from the inner disk accumulate in the outer disk. This process increases the dust-to-gas ratio at large radii. We can ask whether this increase in the dust-to-gas ratio affects the subsequent disk evolution. Suppose that the dust particles inside a radius r are removed and an inner hole (or a gap) is produced. The removed particles pile up in an annulus just outside the inner hole. The width of the annulus is larger than the disk scale height. On the diffusion time t_{rp} , the accumulated particles diffuse over a few disk scale heights both in the vertical and in the radial directions, and during a disk evolution time $t_{\text{out}} > t_{\text{rp}}$, the particles diffuse even further. Thus, the surface density of the annulus increases at most by a factor $\sim \pi r^2 \Sigma_{d,\text{all}} / (2\pi r \Sigma_{d,\text{all}} dr) \lesssim r/h_g \sim 10$, where $dr \gtrsim h_g \sim 0.1r$ is the width of the annulus. Because the gas density does not change, the dust-to-gas ratio of the annulus becomes $\lesssim 10$ times larger. The opacity κ , which is defined for a unit mass of the gas and is proportional to the dust-to-gas ratio, also increases by a factor of order $\lesssim 10$

times. (If the particles diffuse as far as the inner hole radius r in a disk evolution time t_{out} , then the hole is refilled and dust removal is inhibited. The time-scale for the refill is comparable to the gas accretion time-scale r^2/ν , which is shown as the dotted lines in Figure 5. In the standard model, the refill effectively inhibits the dust removal. Only in the high stellar luminosity or the low mass disk cases, the surface outflow can dominate the refill.)

Figure 7 shows how the increase in the dust-to-gas ratio affects the outflow mass flux. In Figure 7, the outflow flux in the cases for $f_{\text{dust}} = 0.1$ (i.e., the dust-to-gas ratio is 10 times larger than the standard model) and for $f_{\text{dust}} = 10^{-3}$ (10 times smaller dust-to-gas ratio) are shown with the standard model. It is seen that the outflow flux depends only weakly on the dust-to-gas ratio. The change in the dust-to-gas ratio has a slight effect on the location of the surface layer, but it hardly changes the dust mass of the surface layer. The thickness of the surface layer is determined so as to make the optical depth be unity, and its mass content does not depend on the dust-to-gas ratio. The variation in the outflow flux arises mainly from change in the location of the surface layer and from change in the angle of the incident starlight to the surface layer, and these effects are small. Therefore, the accumulation of blown off particles increases the dust-to-gas ratio at the disk edge just outside the inner hole, but does not significantly decrease the outflow flux there. Even after the increase in the dust-to-gas ratio in the outer disk, the surface outflow proceeds and the disk evolution continues with the time-scale plotted in Figures 5 and 6.

4.2. Gap Formation in Herbig Ae/Be Disks

The phenomenon of surface stripping can effectively evolve the disk structure around young luminous stars whose luminosity-mass ratios are larger than ~ 15 times the solar value, as shown in §3.4.1. In the outer part ($\gtrsim 200$ AU) of such disks, the surface outflow dominates the inflow through the midplane, causing a net outward flow. On the other hand, within 200 AU, the dust flows inward onto the central star. Around 200 AU, the dust density decreases. The outflow or inflow flux around 200 AU is strong enough that it can carry the total amount of the dust inside 200 AU in 10^7

yr. This flux maintains a relatively constant value throughout the evolution even after the dust density and the dust-to-gas ratio have decreased (see Fig. 7). Consequently, the dust density declines at an almost constant rate. The time-scale for dust diffusion to transport dust from the midplane to replenish the surface layer is about 3×10^6 yr at 200 AU. We expect the dust density at 200 AU will decline considerably in 10^7 yr.

The formation of gaps can be examined by radio observations. At 200 AU, the gas surface density in the standard model is $\Sigma_g = 1.8 \text{ g cm}^{-2}$, which is optically thin in the vertical direction in radio continuum region around 1 mm ($\tau_{1\text{mm}} \sim 10^{-2}$). Therefore, the density decline will be observed as a decrease in the optical depth.

The disk is highly optically thick in the visible or near infrared light ($\tau_{\text{vis}} \sim 200$ at 200 AU). Thus, the density decrease is difficult to examine directly using visible or near-infrared observations. If the gap region is shadowed by the inner disk, or if the edge of the outer disk is illuminated by the central star, the variation in the surface irradiation will probably be observed. There are a few Herbig Ae/Be stars that show gaps in the scattered light images of their disks. The disk around HD 163296 has a dark lane at 325 AU (Grady et al. 2000). HD 100546 also has a disk with a gap at 250 AU (Grady et al. 2001). In order to make direct comparisons with these observations, we need further modeling that takes account of the time evolution of the dust density and that incorporates simulated scattered light images.

In this paper, we discussed gap formation through the surface stripping caused by radiation pressure. It is useful to discuss how to distinguish this mechanism from the other gap formation processes such as the planetary perturbations (Lin & Papaloizou 1986; Takeuchi, Miyama & Lin 1996). Obviously, the surface stripping itself cannot generate non-axisymmetric features, whereas an embedded planet can. In gas-free disks, a planet forms characteristic disk structures that arises from orbital resonances (Roques et al. 1994; Dermott et al. 1994; Liou & Zook 1999; Wyatt et al. 1999; Ozernoy et al. 2000; Wilner et al. 2002; Quillen & Thorndike 2002), and in gas disks the planet excites spiral density waves (Miki 1982; Sekiya, Miyama, & Hayashi 1987; Bryden et al. 1999; Kley 1999; Lubow, Seibert, & Artymowicz

1999; Miyoshi et al. 1999; Tanigawa & Watanabe 2002). The detection of such non-axisymmetric features would rule out surface stripping as a gap formation mechanism. The other notable feature of surface stripping is that it does not affect the gas density structure. The gas disks still have monotonic density structure even after the dust disks have formed gaps. Therefore, detection of gaps in gas disks also rules out surface stripping. In order to explain the cause of the gaps around HD 163296 and HD 100546, it is important to determine with future observations whether their gas disks have gaps or not.

4.3. Summary

Dust particles that are directly irradiated by the star move outward under the combined action of gas drag and radiation pressure. In this paper, the surface outflow of particles in optically thick disks is studied. Our results are as follows.

1. Particles in the surface layer, which are directly exposed to the starlight, move outward. In a disk resembling the minimum-mass-solar-nebula, the height of the surface layer is about three scale heights of the gas disk and the mass is 10^{-6} times the total dust mass at 1 AU and 10^{-4} times the total dust mass at 100 AU. For this case, the mass flux of the surface outflow is much smaller than the inflow mass flux inside the disk, and the surface outflow does not contribute significantly to the dust disk evolution.

2. The surface outflow dominates the inflow in the following cases: (a) If the luminosity-mass ratio of the central star is 15 times larger than the solar value, the velocity of the surface outflow is large enough at the outer part of the disk ($r \gtrsim 200$ AU). (b) If the mass of the gas disk is as small as 10^{-2} times the minimum-mass disk ($\sim 100M_{\oplus}$ inside 100 AU), the mass ratio of the surface layer to the whole dust disk is large enough at a few tens AU. In such cases, the surface outflow induces formation of gaps or rings.

3. The surface outflow is mainly composed of particles with size of order $\sim 0.1 \mu\text{m}$. As the particles grow, the largest particles around the midplane move inward more rapidly, while the outflow flux at the surface remains at a near-constant value. This results in a diminishing importance of the surface outflow for the overall disk evolution.

We would like to thank the referee for helpful comments. We also thank Greg Laughlin for his careful reading the manuscript and correcting grammar. This work was supported in part by an NSF grant AST 99 87417 and in part by a special NASA astrophysical theory program that supports a joint Center for Star Formation Studies at UC Berkeley, NASA-Ames Research Center, and UC Santa Cruz. This work is also supported by NASA NAG5-10612 through its Origin program and by JPL 1228184 through its SIM program.

REFERENCES

- Adachi, I., Hayashi, C., & Nakazawa, K. 1976, *Prog. Theor. Phys.* 56, 1756
- Balbus, S. A., & Hawley, J. F. 1991, *ApJ*, 376, 214
- Beckwith, S. V. W., & Sargent, A. I. 1991, *ApJ*, 381, 250
- Bryden, G., Chen, X., Lin, D. N. C., Nelson, R. P., & Papaloizou, J. C. B. 1999, *ApJ*, 514, 344
- Cuzzi, J. N., Dobrovolskis, A.R., & Champney, J. M. 1993, *Icarus*, 106, 102
- D'Alessio, P., Calvet, N., & Hartmann, L. 2001, *ApJ*, 553, 321
- D'Antona, F., & Mazzitelli, I. 1994, *ApJS*, 90, 467
- Dermott S. F., Jayaraman, S., Xu, Y. L., Gustafson, B. A. S., & Liou, J. C., 1994, *Nature*, 369, 719
- Grady, C. A., et al. 2000, *ApJ*, 544, 895
- Grady, C. A., et al. 2001, *AJ*, 122, 3396
- Hartmann, L., Calvet, N., Gullbring, E., & D'Alessio, P. 1998, *ApJ*, 495, 385
- Hellyer, B. 1970, *MNRAS*, 148, 383
- Klahr, H. H., & Lin, D. N. C. 2001, *ApJ*, 554, 1095
- Kley, W. 1999, *MNRAS*, 303, 696
- Lin, D. N. C., & Papaloizou, J. C. B. 1980, *MNRAS*, 191, 37
- Lin, D. N. C., & Papaloizou, J. C. B. 1986, *ApJ*, 307, 395
- Liou, J. -C., & Zook, H. A. 1999, *AJ*, 118, 580
- Lubow, S. H., Seibert, M., & Artymowicz, P. 1999, *ApJ*, 526, 1001
- Mannings, V., & Emerson, J. P. 1994, *MNRAS*, 267, 361
- Miki, S. 1982, *Prog. Theor. Phys.*, 67, 1053
- Miyake, K., & Nakagawa, Y. 1993, *Icarus*, 106, 20
- Miyoshi, K., Takeuchi, T., Tanaka, H., & Ida, S. 1999, *ApJ*, 516, 451
- Monin, A. S., & Yaglom, A. M. 1971, *Statistical Fluid Mechanics: Mechanics of Turbulence*, Volume 1 (Cambridge: The MIT Press), Ch. 10
- Morfill, G. E. 1985, in *Birth and Infancy of Stars*, eds. R. Lucas, A. Omont, & R. Stora (Amsterdam: Elsevier Science Publishers), 693
- Ozernoy, L. M., Gorkavyi, N. N., Mather, J. C., & Taidakova, T. A., 2000, *ApJ*, 537, L147
- Quillen, A. C., & Thorndike, S. 2002, *ApJ*, 578, L149
- Roques, F., Scholl, H., Sicardy, B., & Smith, B. A. 1994, *Icarus*, 108, 37
- Sekiya, M., Miyama, S. M., & Hayashi, C. 1987, *Earth, Moon, and Planets*, 39, 1
- Shakura, N. I., & Sunyaev, R. A. 1973, *A&A*, 24,337
- Takeuchi, T., & Artymowicz, P. 2001, *ApJ*, 557, 990
- Takeuchi, T., & Lin, D. N. C. 2002, *ApJ*, 581, 1344 (Paper I)
- Takeuchi, T., Miyama, S. M., & Lin, D. N. C. 1996, *ApJ*, 460, 832
- Tanigawa, T., Watanabe, S. 2002, *ApJ*, 580, 506
- Weidenschilling, S. J. 1977, *MNRAS*, 180, 57
- Weidenschilling, S. J., & Cuzzi, J. N. 1993, in *Protostars and Planets III*, ed. E. H. Levy & J. I. Lunine (Tucson:Univ. of Arizona Press), 1031
- Wilck, M., & Mann, I. 1996, *Planet. Space Sci.*, 44, 493
- Wilner, D. J., Holman, M. J., Kuchner, M. J., & Ho, P. T. P. 2002, *ApJ*, 569, L115
- Wyatt, M. C., Dermott, S. F., Telesco, C. M., Fisher, R. S., Grogan, K., Holmes, E. K., & Piña, R. K. 1999, *ApJ*, 527, 918

This 2-column preprint was prepared with the AAS L^AT_EX macros v5.0.

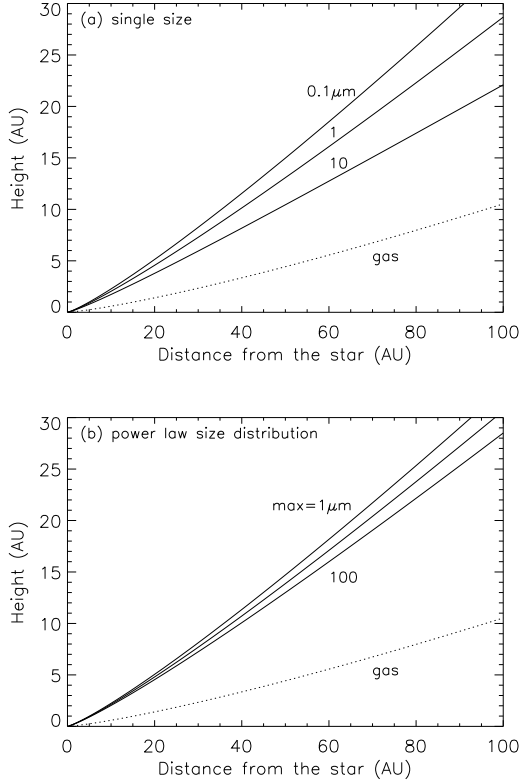


Fig. 1.— Locations of the illuminated surfaces. (a) The dust particles are assumed to be single-sized. The sizes are 0.1, 1, and 10 μm from the upper line. The dotted line shows the scale height of the gas disk. (b) The size distribution is a power-law with an index -3.5 . The minimum size is 0.01 μm . The maximum sizes are 1, 10, and 100 μm from the upper line.

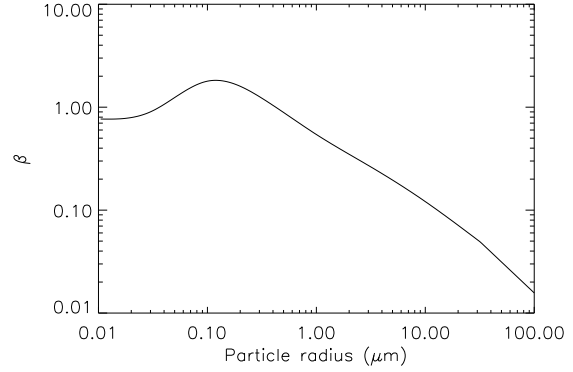


Fig. 2.— Radiation pressure to gravity ratio β of the “young cometary particles.” The value is from Wilck & Mann (1996).

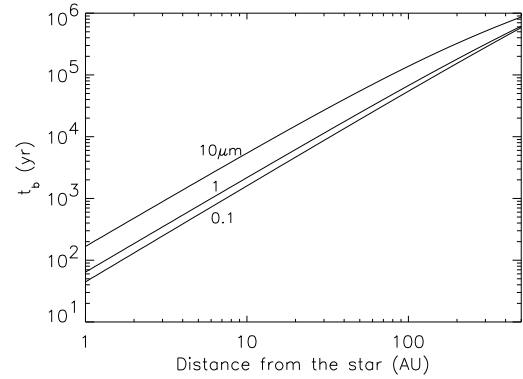


Fig. 3.— Blow-off time of the outflowing particles in the surface layer. The particles are single-sized of 10, 1, and 0.1 μm from the upper line.

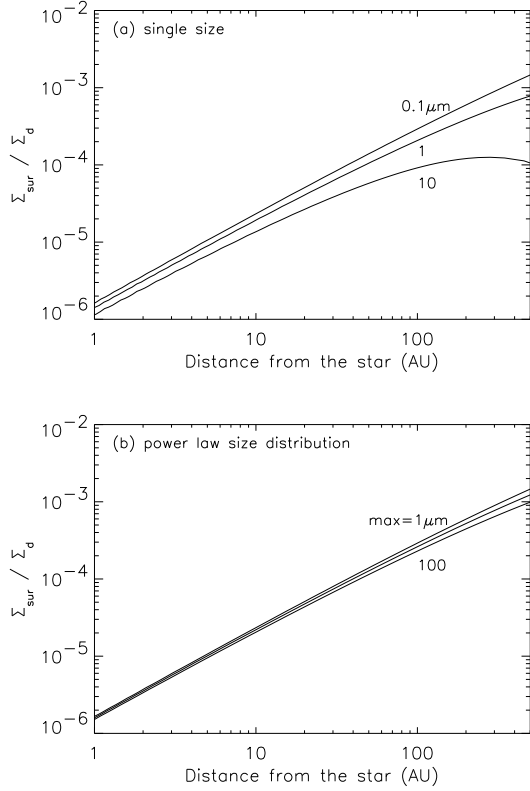


Fig. 4.— Mass ratio of the surface layer above the illuminated surface to the whole dust disk ($\Sigma_{d,\text{sur,all}}/\Sigma_{d,\text{all}}$). (a) The dust particles are single-sized. The sizes are 0.1, 1, and 10 μm from the upper line. (b) The size distribution is a power-law with an index -3.5 . The minimum size is 0.01 μm . The maximum sizes are 1, 10, and 100 μm from the upper line.

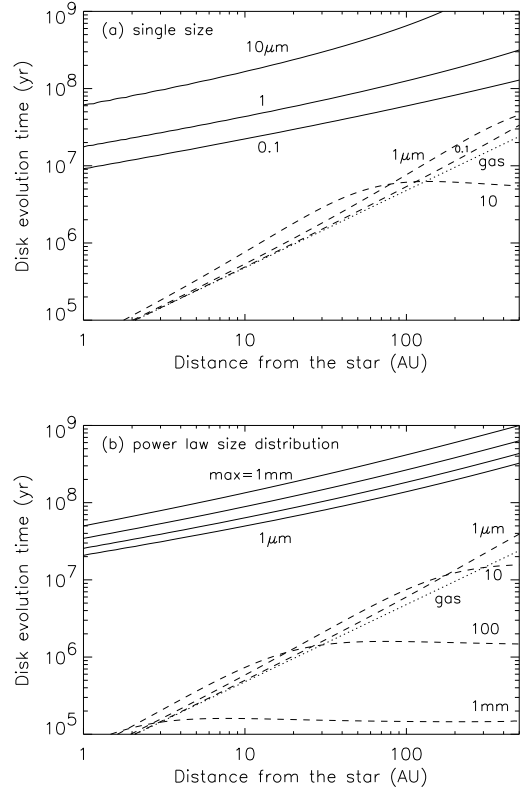


Fig. 5.— Disk evolution time through the outflow and the inflow. The solid lines show the evolution time through the surface outflow, and the dashed lines show the evolution time through the inflow inside the disk. The dotted line shows the accretion time-scale of the gas. (a) The particles are single-sized. The sizes are 10, 1, and 0.1 μm from the upper lines (at 10 AU for the dashed lines). (b) The size distribution is a power-law with an index -3.5 and a minimum size 0.01 μm . The maximum sizes are 1 mm, 100, 10, and 1 μm from the upper solid line and from the lower dashed line.

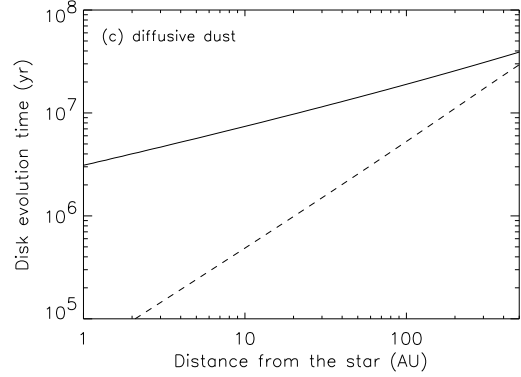
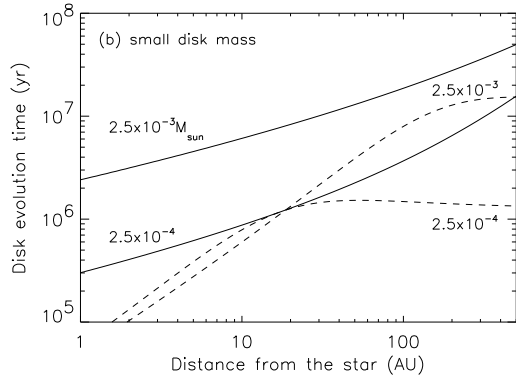
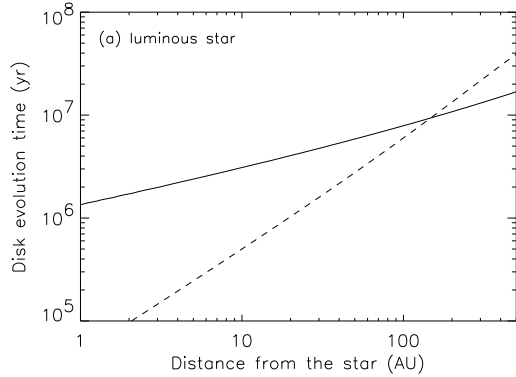


Fig. 6 — continued

Fig. 6.— Disk evolution time for various models. The solid and dashed lines correspond to the evolution time through the surface outflow and through the inflow inside the disk, respectively. Particles have a power-law size distribution with $s_{\text{max}} = 1 \mu\text{m}$. Parameters are the same as the standard model except for: (a) The luminosity-mass ratio of the central star is $L/M = 15L_{\odot}/M_{\odot}$. (b) The disk is less massive. The gas masses inside 100 AU are $2.5 \times 10^{-3}M_{\odot}$ and $2.5 \times 10^{-4}M_{\odot} = 83M_{\oplus}$ from the upper line. (c) The particles are more diffusive ($Sc = 0.1$).

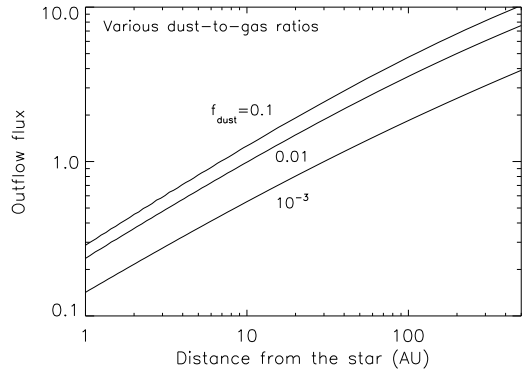


Fig. 7.— Surface dust flux for various dust-to-gas ratios, $f_{\text{dust}} = 0.1, 0.01, \text{ and } 10^{-3}$ from the upper line. The flux is normalized by the value of the standard model ($f_{\text{dust}} = 0.01$) at 10 AU.